# Microstructure and Rheologic Development of Polypropylene/Nano-$CaCO_3$ Composites along Twin-Screw Extruder

**Guo Jiang, Han-Xiong Huang**

*Laboratory for Micro Molding and Polymer Rheology, College of Industrial Equipment and Control Engineering, South China University of Technology, Guangzhou, People's Republic of China*

Received 4 February 2008; accepted 26 December 2008
DOI 10.1002/app.30186
Published online 24 June 2009 in Wiley InterScience (www.interscience.wiley.com).

**ABSTRACT:** Polypropylene/nano-calcium carbonate (PP/nano-$CaCO_3$) composites were prepared by using an intermeshing, co-rotating twin-screw extruder. Two different screw configurations, denoted by screws A and B, respectively, were employed. The former provided high dispersive mixing and the later provided high dispersive and distributive mixing. Effect of mixing type on microstructure and rheologic development of nanocomposites was investigated by taking samples from four locations along screws A and B. Transmission electron microscopy results show that in the sample at the exit of extruder, the percentage of nano-$CaCO_3$ particles with the equivalent diameter lower than 100 nm along screws A and B is 66.5 and 79.0%. respectively. Moreover, for screw B, the number-averaged diameter at four sampling locations is smaller than that for screw A. This means that the distributive mixing, provided by screw B, favors the size decrease of nano-$CaCO_3$ in the PP matrix. In addition, rheologic results show that the decrease of complex viscosity for the nanocomposites is deeply related to turbine mixing elements, which provides distributive mixing. The online melt shear viscosity of the nanocomposite at the exit of extruder prepared by screw B is lower than that of pure PP. This is related to the dispersion of nano-$CaCO_3$ in PP matrix. Finally, the relationship between rheologic properties and microstructure was analyzed. © 2009 Wiley Periodicals, Inc. J Appl Polym Sci 114: 1687–1693, 2009

**Key words:** extrusion; microstructure; mixing; nanocomposites; rheology

## INTRODUCTION

Polymer nanocomposites have been extensively investigated owing to their improved mechanical and electrical properties, heat resistance, radiation resistance, and other properties as a result of the nanometric scale dispersion of particles in polymer matrix.[1] The investigation of polymer/nano-calcium carbonate ($CaCO_3$) composite is one of the most active areas.[2–7] Many efforts have been devoted to improve the dispersion of the nano-$CaCO_3$ in the polymer matrix.[8–10]

Extruders are widely used to prepare polymer nanocomposites and blends. The morphology of polymer nanocomposites or blends is deeply related to the flow field during the processing. The research by Huang et al. showed that the type of the mixing and the intensity of the shear in the extruder screw exhibit a distinct influence on the microstructure of the polypropylene (PP)/organic montmorillonite (OMMT) nanocomposite[11] or polymer blends[12,13] prepared by direct melt intercalation or melt blending. In previous works by this laboratory,[14–16] the effect of screw configuration on the microstructure of the PP/nano-$CaCO_3$ composite at the exit of the twin-screw extruder was studied. Read et al. investigated the development of microstructure for a melt-blended PP/OMMT nanocomposite along a co-rotating intermeshing twin-screw extruder.[17] They suggested that the final dispersion level at the smallest scale is reached in the first melting section but is not reduced with additional shear or residence time.

Recently, rheologic analysis is considered as an effective tool to investigate the microstructure of polymer nanocomposites.[18–20] However, there exist different results about the effect of nanoparticles on the rheologic behavior of polymer/nano-$CaCO_3$ composites. For example, for the polymer/nano-$CaCO_3$ composites, the research by Wu et al. showed that the addition of nano-$CaCO_3$ particles into polyvinyl chloride (PVC) results in a remarkable increase of the melt viscosity.[21] However, Xie et al. reported that the apparent viscosity of PVC/$CaCO_3$ nanocomposites decreases with increasing nanoparticle

*Correspondence to:* H.-X. Huang (mmhuang@scut.edu.cn).
Contract grant sponsor: National Natural Science Foundation of China; contract grant number: 10272048.
Contract grant sponsor: Higher Education Institutions of MOE, People's Republic of China.

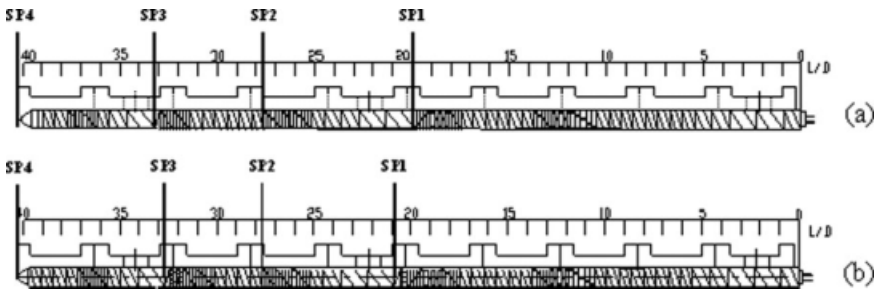


**Figure 1** Configurations for screws (a) A and (b) B and sampling locations.

content and is lower than that of pristine PVC at high shear rate (>100 $s^{-1}$).[22] In their studies, the melt shear viscosity of nanocomposites was measured by using a rheometer offline.

For the aforementioned reasons, the objective of this work was to investigate the effect of the dispersive and distributive mixing on the microstructure and rheologic development of PP/nano-$CaCO_3$ composite along a twin-screw extruder. The online melt shear viscosity of the nanocomposite at the end of extruder during the compounding and the dynamical rheologic properties of the samples taken along the twin-screw extruder were measured. Moreover, the relationship between the microstructure and rheologic properties of the nanocomposite was analyzed.

## MATERIALS AND METHODS

### Materials

The polymer matrix was PP (J501, Sinopec Group Guangzhou, China) with a melt index of 2.7 g/10 min (230°C and 2.16 kg). The nano-$CaCO_3$ was manufactured by Inner Mongolia Mengxi, China. This nano-$CaCO_3$ was pretreated by the manufacturer and its mean size was 30 nm. Stearic acid was used as coupling agent. The content of the coupling agent was 1.5 wt % of the nano-$CaCO_3$.

### Sample preparation

The PP/nano-$CaCO_3$ composites were compounded by using a modular co-rotating, intermeshing twin-screw extruder with a screw diameter of 35 mm and a length–diameter ratio of 40 : 1. The screw elements were selected and arranged to provide high mixing. Two different screw configurations employed in this work were denoted by screws A and B, respectively. As shown in Figure 1, in screw A, five kneading block sections were used to impose high shear intensity. A reverse kneading block was set in the second kneading block section to increase the filled degree of the screw elements. Two neutral kneading elements set in the first and second kneading block sections favored the melting of the polymer. A left-handed screw element was set at the fourth kneading block section to extend the residence time of polymer melts. In screw B, turbine mixing elements were set after the second and fourth kneading block sections to enhance the distributive mixing.

The nano-$CaCO_3$ was dried in an oven at 90°C for 4 h and then mixed with the coupling agent for about 10 min to facilitate the dispersion of the nanoparticles in the PP matrix. The PP and the nano-$CaCO_3$ particles with the weight ratio of 90/10 were dry-mixed thoroughly before feeding into the twin-screw extruder. The compounding was carried out at temperature profiles of 160-180-195-195-190-190-190-190-190°C from the hopper to the strand die. The screw speed was set at 400 rpm.

The sample at location SP4 (shown in Fig. 1) was taken at the exit of the extruder when the extrusion was at the steady state. The screws were dragged out when the extruder was stopped by means of the emergency stop button. Then the samples were taken from different locations (SP1 to SP3, shown in Fig. 1) along the screws.

### Microstructure observation

Ultra-thin films with about 100 nm in thickness were cut from the samples in a nitrogen environment. Transmission electron microscopy (TEM; Jeol JEM-100CX II), operated at an accelerating voltage of 100 kV, was used to observe the microstructure of the samples. The size distribution of nanoparticles was quantitatively determined by analyzing the TEM photomicrographs by using Scion image software (Beta 4.02, Scion Corp.). The obtained area values ($A_d$) of dispersed particles were used to calculate the equivalent diameter ($d$)

$$d = \sqrt{4A_d/\pi}. \quad (1)$$

From the so-obtained equivalent diameters, the number-averaged diameter ($d_n$) was determined as

$$d_n = \sum_{i=1}^{n} d_i/n, \quad (2)$$

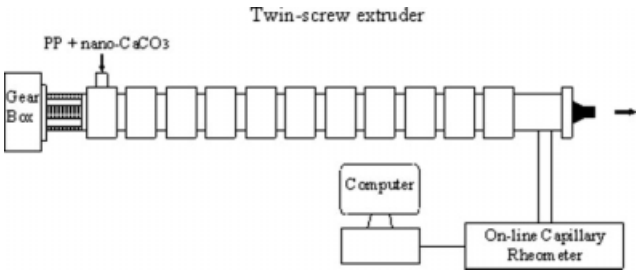


**Figure 2** Schematic of online shear viscosity measurement and the extrusion process to prepare nanocomposites.

where $n$ is the number of counted particles. At least three TEM photomicrographs were analyzed for sample taken from each location.

### Rheologic behavior measurement

The dynamic rheologic properties of above-taken samples were measured by using a Bohlin Gemini 200 Rheometer System, with a parallel plate geometry using 25-mm diameter plates at 190°C. The disks, with a size of $\phi$25 mm $\times$ 1 mm, were compression molded from the samples taken from four locations along screw B. The sweep range of frequency ($\omega$) was from 0.01 to 50 rad/s using the strain level of 1% to ensure that the measurement was carried out in the linear viscoelastic region of nanocomposite.

The capillary rheometer, Haake ProFlow online rheometer, was used to measure the melt shear viscosity of nanocomposites at the exit of extruder. The ProFlow system continuously diverted a small flow of material from the end of the extruder and pushed the material through a capillary by means of a melt pump. The pressure before the melt pump was controlled by an automatic bypass valve to avoid the disturbance of the process during the measurement. In this work, the online rheometer was side-mounted at the end of the twin-screw extruder (shown in Fig. 2) and the melt shear viscosity of nanocomposite was measured during the compounding.

## RESULTS AND DISCUSSION

The TEM photomicrographs for the samples collected from four locations along screws A and B are

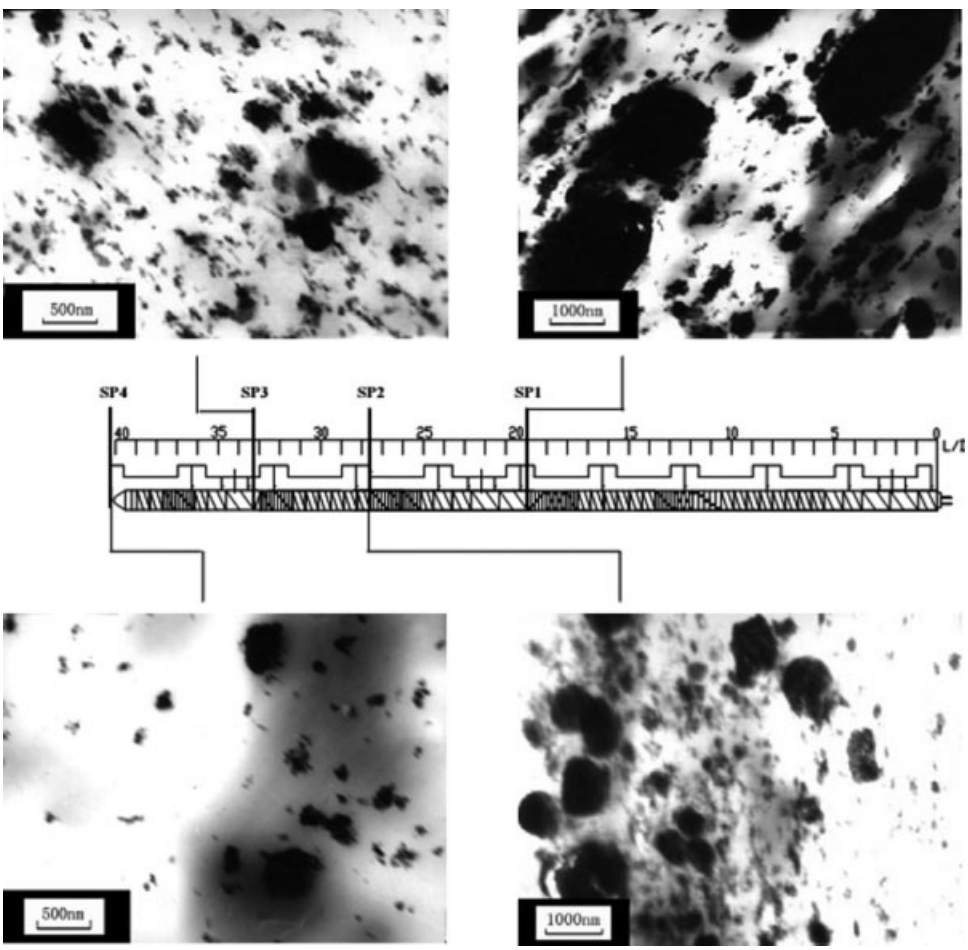


**Figure 3** TEM photomicrographs of samples taken from four locations along screw A.

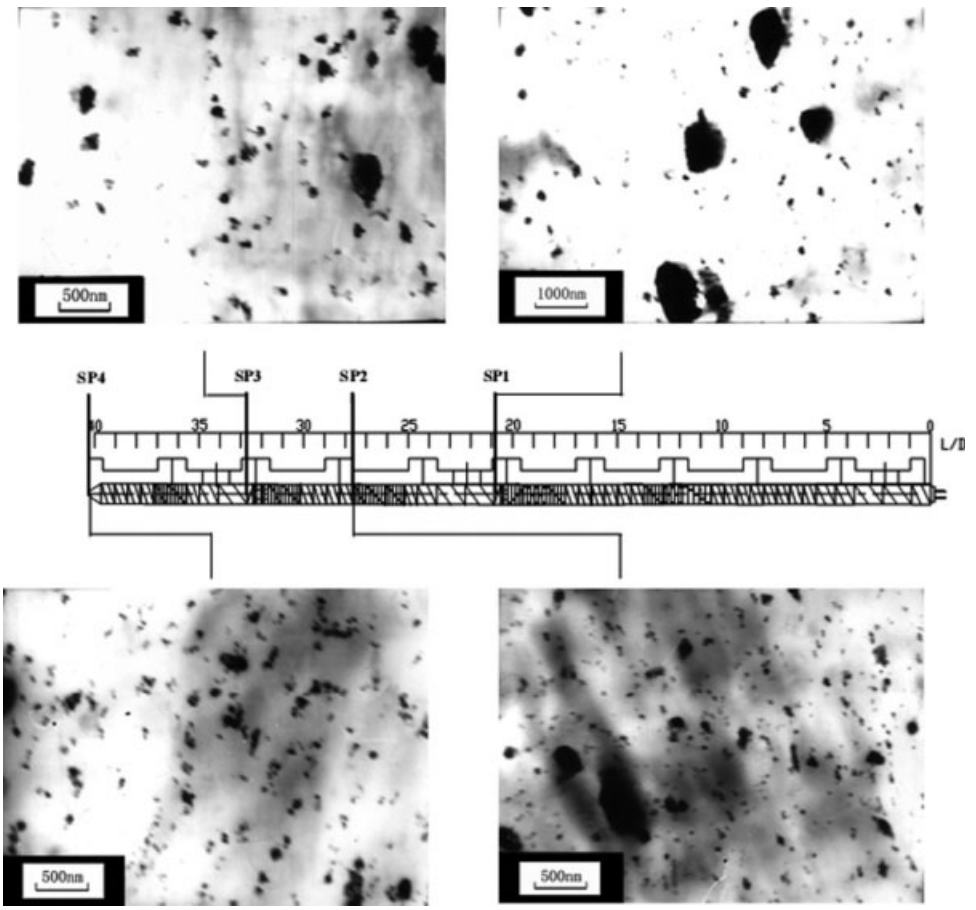


**Figure 4** TEM photomicrographs of samples taken from four locations along screw B.

shown in Figures 3 and 4, respectively. As can be clearly seen, the size of the nano-$CaCO_3$ decreases gradually along screws A and B. It is obviously observed that the size of nanoparticles for the nanocomposite prepared by screw B is much smaller than that prepared by screw A.

The number-averaged diameter ($d_n$) and the largest diameter ($d_{max}$) of nano-$CaCO_3$ particles in the samples collected from four locations are shown in Figures 5 and 6, respectively. Figure 7 illustrates the percentage of nano-$CaCO_3$ particles with the equivalent diameter lower than 100 nm (Φ) in the samples

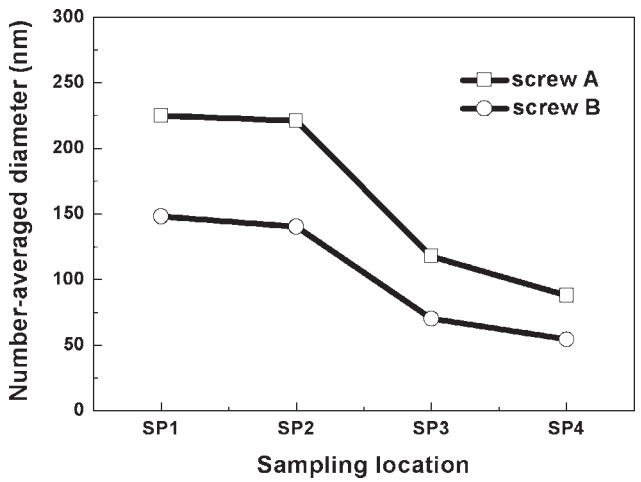


**Figure 5** The number-averaged diameter of nano-$CaCO_3$ particles in samples taken from four locations along screws A and B.

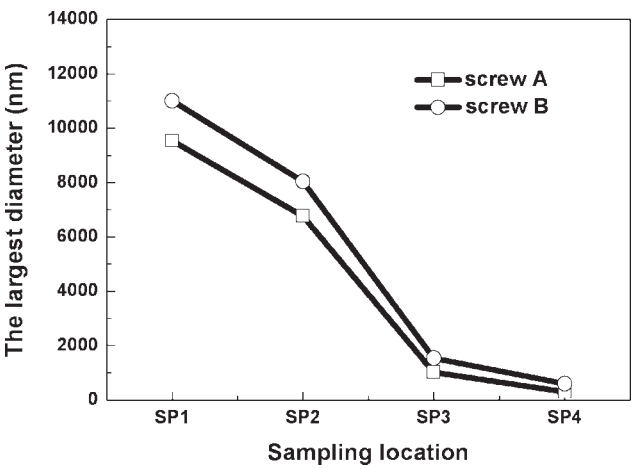


**Figure 6** The largest diameter of nano-$CaCO_3$ particles in samples taken from four locations along screws A and B.

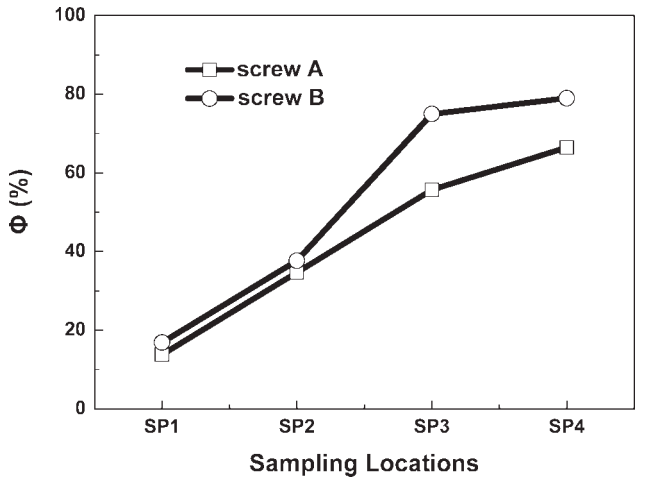


**Figure 7** The Φ (percentage of nano-$CaCO_3$ particles with the equivalent diameter lower than 100 nm) for samples taken from four locations along screws A and B.

collected from four locations. For screw A, as shown in Figures 5, 6, and 7, the $d_n$ of nano-$CaCO_3$ decreases from 225 nm (SP1) to 88 nm (SP4). The $d_{max}$ decreases from 11,000 nm (SP1) to 8039 nm (SP2), 1541 nm (SP3), and 600 nm at the exit (SP4). The Φ is increased from 13.8% (SP1) to 66.5% (SP4). Moreover, the increase of Φ from SP2 to SP3 is larger than that from SP3 to SP4. This is related to the screw configurations. At SP3, a left-handed conveying screw element was set. Generally speaking, a left-handed screw element, having a negative pitch, can build negative pressure gradient. This means a longer residence time through this type of screw element. With the increase of residence time, the mixing time for the nanocomposites is increased and to some extent this may facilitate the dispersion of nano-$CaCO_3$ in PP matrix.

For screw B, as can be seen from Figures 5 and 6, the $d_n$ and $d_{max}$ of nano-$CaCO_3$ is smaller than that for screw A. At SP4, the $d_n$ is 54 nm. The $d_{max}$ is decreased from 9531 nm (SP1) to 6770 nm (SP2), 1020 nm (SP3), and 300 nm at the end (SP4). As shown in Figure 7, the Φ is increased from 16.9% (SP1) to 37.7% (SP2), 75.0% (SP3), and 79.0% (SP4).

For polymer nanocomposites with the same composition, the processing conditions are the most important factors to affect their microstructure. In this work, the processing parameters, such as temperature of the extruder and rotating speed of screws, are kept constant. So the mixing type and intensity during the compounding become key factors affecting the dispersion of nano-$CaCO_3$ in PP matrix. Compared with the configuration of screw A, turbine mixing elements (TMEs) and left-handed screw element are set in SP1 and SP3 for screw B. TMEs can provide distributive mixing.[23] These elements are defined by the number of teeth around the circumference and the tooth angle. The quantitative analysis on TEM photomicrographs (shown in Figs. 3 and 4) shows that the Φ at SP1 along screw B, 16.9%, is higher than that at SP1 along screw A, 13.8%. From SP2 to SP3, the increase of Φ for screw B is larger than that for screw A (shown in Fig. 7). This means that the TMEs with higher distributive mixing favor the size decrease of nano-$CaCO_3$.

Figure 8 presents the dynamical rheologic properties of the samples taken at four locations along screw B. As can be seen, storage modulus ($G'$) and loss modulus ($G''$) decrease little from locations SP1 to SP2 and are slightly larger from SP3 to SP4. Similarly, the complex viscosity (η*) decreases from SP1 to SP4. The decrease of η* from SP1 to SP2 is small, whereas its decrease becomes larger from SP3 to SP4. Xie et al.[22] proposed that spherical nano-$CaCO_3$ particles serve as "ball bearing," reducing the interlayer interaction of PVC melts and thereby decreasing the viscosity of the polymer matrix. The microstructure development of samples along the extruder can be used to analyze the development of their dynamic rheologic properties. With the melt flow from locations SP1 to SP4 along screw B, the size of the nano-$CaCO_3$ particles gradually becomes small. The hindering of the nanoparticles to the polymer melt flow becomes weaker and the melt is easier to flow. So the complex viscosity of samples decreases along the twin-screw extruder. In addition, it is shown that the decreases of $G'$, $G''$, and η* from SP1 to SP2 are small, whereas the decreases become larger from SP2 to SP3 and SP3 to SP4. This may be explained by the change of the $d_n$ of nano-$CaCO_3$ in samples taken from SP1 to SP4. The $d_n$ decreases little from SP1 to SP2. From SP2 to SP3, the $d_n$ decreases largely (from 140.3 to 70.2 nm), which results in a slightly larger decrease of η*. As presented in Figure 1, turbine mixing elements are set between locations SP2 and SP3. This indicates that a much larger decrease of complex viscosity for PP/nano-$CaCO_3$ composites is deeply related to turbine mixing elements, which provides distributive mixing.

In addition, the online shear viscosity of the nanocomposites was measured at the exit of the extruder. Figure 9 presents the shear viscosity versus shear ratio curves of nanocomposites and pure PP. As can be seen from Figure 9, the shear viscosity of the nanocomposite prepared by screw A is higher than that of pure PP, whereas the shear viscosity of nanocomposite prepared by screw B is lower than that of pure PP. This can be explained on the basis of the rheologic behavior and microstructure observation of nanocomposites. The Φ and $d_n$ of $CaCO_3$ particles are used to characterize the dispersion of nanoparticles in PP matrix. If there exist more nanoparticles with the equivalent diameter lower than 100 nm (higher Φ) in PP matrix, these nano-$CaCO_3$ may

be served as lubricant, decreasing the viscosity of PP/nano-$CaCO_3$ composites. Lower Φ means that there exists more aggregations with large diameter and they serve as rigid particles. These rigid nanoparticles may hinder the flow of the melt and then the viscosity increases. In our previous work,[16] it was preliminarily deduced that there exists a critical percentage of nano-$CaCO_3$ with the equivalent diameter lower than 100 nm ($\Phi_{cr}$) or a critical equivalent diameter ($d_{cr}$). For the PP/nano-$CaCO_3$ composite, the $\Phi_{cr}$ is about 80% and $d_{cr}$ is about 60 nm. In this work, microstructure results show that for the nanocomposite prepared by screw B, nearly 80% nanoparticles have the equivalent diameter lower than 100 nm and the final $d_n$ is 54 nm. The Φ is higher than $\Phi_{cr}$ and the $d_n$ is lower than $d_{cr}$. So the shear viscosity of the nanocomposite prepared by screw B is lower than that of pure PP. For the nanocomposite prepared by screw A, there is 66.5% nanoparticles with the equivalent diameter lower than 100 nm and the final $d_n$ of nanoparticles is 88 nm. The Φ is lower than $\Phi_{cr}$ and the $d_n$ is higher than $d_{cr}$. So the shear viscosity is higher than that of pure PP.

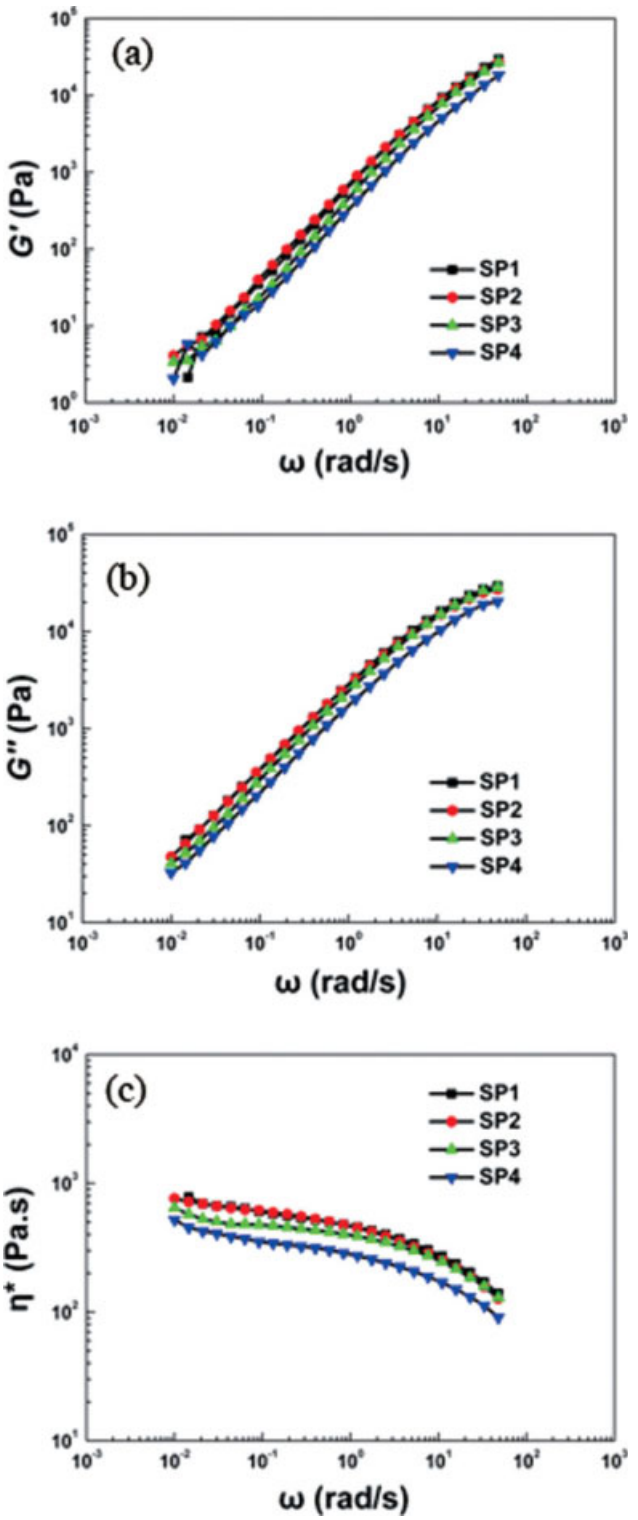


**Figure 8** (a) Storage modulus, (b) loss modulus, and (c) complex viscosity of samples taken from four locations along screw B. [Color figure can be viewed in the online issue, which is available at www.interscience.wiley.com]

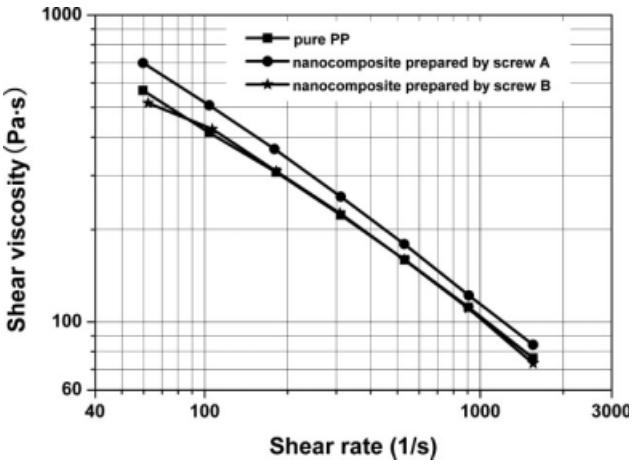


**Figure 9** Online shear viscosity of pure PP and the nanocomposites prepared by screws A and B.

## CONCLUSIONS

Microstructure and rheologic property development of the PP/nano-$CaCO_3$ composite along a twin-screw extruder was investigated. Two different screw configurations, denoted by screws A and B, respectively, were employed. The former provided high dispersive mixing and the latter provided high dispersive and distributive mixing. TEM results show that in the samples collected at the exit of the extruder, the percentage of nanoparticles with the equivalent diameter lower than 100 nm along screws A and B is 66.5% and 79.0%, respectively. It is deduced that the distributive mixing facilitates the dispersion of the nanoparticles in the composite. In addition, the storage modulus, loss modulus, and complex viscosity of the samples decrease from the first sampling location to the exit of the extruder.

The online shear viscosity of the nanocomposite at the exit of extruder prepared by screw B is lower than that of pure PP. The rheologic behaviors are deeply related to the microstructure of nanocomposite. It is deduced that there exists a critical percentage of nano-$CaCO_3$ particles with the equivalent diameter lower than 100 nm or a critical number-averaged diameter, which affects the melt shear viscosity of nanocomposite. For PP/nano-$CaCO_3$ composites, the critical percentage and number-averaged diameter is 80% and 60 nm, respectively.

## References


1. Alexandre, M.; Dubois, P. Mater Sci Eng R Rep 2000, 28, 1.
2. Zuiderduin, W. C. J.; Westzaan, C.; Huétink, J.; Gaymans, R. J. Polymer 2003, 44, 261.
3. Chan, C. M.; Wu, J. S.; Li, J. X.; Cheung, Y. K. Polymer 2002, 43, 2981.
4. Levita, G.; Marchetti, A.; Lazzeri, A. Polym Compos 1989, 10, 39.
5. Hong, C. H.; Lee, Y. B.; Bae, J. W.; Jho, J. Y.; Nam, B. U.; Hwang, T. W. J Appl Polym Sci 2005, 98, 427.
6. Zhang, Y.; Chan, C. M.; Wu, J. S. SPE ANTEC Tech Pap 2004, 50, 1795.
7. Deshmane, C.; Yuan, Q.; Misra, R. D. K. Mater Sci Eng A 2007, 452, 592.
8. Di Lorenzo, M. L.; Errico, M. E.; Avella, M. J Mater Sci 2002, 37, 2351.
9. Khunova, V.; Hurst, J.; Janigova, I.; Smatko, V. Polym Test 1999, 18, 501.
10. Zhang, H.; Chen, J. F.; Zhou, H. K.; Wang, G. Q.; Yun, J. J Mater Sci Lett 2002, 21, 1305.
11. Huang, H. X.; Huang, Y. F.; Wang, C. Y.; Zhang, Y. H. J Mater Sci Lett 2003, 22, 1547.
12. Huang, H. X.; Huang, Y. F.; Yang, S. L. Polym Int 2005, 54, 65.
13. Huang, H. X. J Mater Sci 2005, 40, 1777.
14. Huang, H. X.; Jiang, G.; Mao, S. Q. Am Soc Mech Eng 2005, 567.
15. Huang, H. X.; Jiang, G.; Mao, S. Q. J Mater Sci 2006, 41, 4985.
16. Jiang, G.; Huang, H. X. J Mater Sci 2008, 43, 5305.
17. Read, M. D.; Liu, L.; Harris, J. D.; Samson, R. R. SPE ANTEC Tech Pap 2004, 50, 1882.
18. Chow, W. S.; Mohd Ishak, Z. A.; Karger-Kocsis, J. Macromol Mater Eng 2005, 290, 122.
19. Li, J.; Zhou, C. X.; Wang, G.; Zhao, D. J Appl Polym Sci 2003, 89, 3609.
20. Jiang, L.; Lam, Y. C.; Tam, K. C.; Chua, T. H.; Sim, G. W.; Ang, L. S. Polymer 2005, 46, 243.
21. Wu, D. Z.; Wang, X. D.; Song, Y. Z.; Jin, R. G. J Appl Polym Sci 2004, 92, 2714.
22. Xie, X. L.; Liu, Q. X.; Li, R. K. Y.; Zhou, X. P.; Zhang, Q. X.; Yu, Z. Z.; Mai, Y. W. Polymer 2004, 45, 6665.
23. Burbank, F.; Baruer, F.; Andersen, P. SPE ANTEC Tech Pap 1991, 37, 149.